UNSTRUCTURED GRID METHODS FOR THE SIMULATION OF 3D TRANSIENT FLOWS

Final Report for the Period : 1 January 1992– 31 December 1993

Prepared for the
Dryden Flight Research Facility
NASA Ames Research Center
Post Office Box 273
Edwards
California 93523, U.S.A.

NASA RESEARCH GRANT No. NAGW—2962

Technical Monitor : K.K. Gupta

Principal Investigator : K. Morgan
Co–Investigators : J. Peraire & J. Peiró

Submitted by the
Department of Civil Engineering
University of Wales Swansea
Singleton Park
Swansea SA2 8PP
United Kingdom

Report Prepared: 1st June 1994

1. INTRODUCTION

This report gives a description of the work which has been undertaken at the University of Wales Swansea under NASA Research Grant NAGW—2962. The objective of the research program was to produce an initial capability for the efficient simulation of 3D transient inviscid compressible flows on unstructured tetrahedral meshes. There was also an objective of investigating the simulation of flows involving oscillating boundaries.

2. WORK ACCOMPLISHED

Over the past ten years, the views of the aerospace industry on the use of unstructured grid methods for the simulation of aerodynamic flows have changed considerably. In the early eighties, these methods were greeted with a large degree of suspicion. At that time, the main causes for concern were the perceived difficulty of generating unstructured grids of high quality and the question of the accuracy of the results of computations made on general unstructured grids. In the intervening period, researchers have made major strides in the areas of grid generation, accuracy and adaptivity so that, nowadays, most major aerospace companies have, or are working towards the acquisition of, an unstructured grid aerodynamics capability. In addition, it is already recognised by industrial users that the unstructured approach will have an important role to play in the development of any successful multi-disciplinary (i.e. fluid dynamics, electro-magnetics, structural mechanics, optimisation) analysis capability (Shankar, Hall, Mohammadian and Rowell 1993).

We will begin by oulining a general framework for the development of algorithms for the solution of the inviscid flow equations on general unstructured tetrahedral grids. The approach which will be followed employs an edge based representation of the grid. It will be shown that, as well as being a convenient mechanism for algorithm development, the edge based representation has significant implications to the computational efficiency of the flow solvers, both in terms of computer time and memory requirements. Practical algorithms which have been utilised to date for the simulation of steady flows are generally based upon the use of explicit time stepping methods. In the structured grid context, more efficient methods have been developed which are based upon explicit time stepping with multigrid acceleration (Jameson 1983). However, the implementation of the multigrid idea within the unstructured grid environment is not straightforward and certain difficulties need to be overcome. The use of explicit methods for the simulations of truly transient flows can lead to significant computational requirements. The extension of the multigrid approach to handle transient problems is considered and the method is employed in the analysis of the flow over an oscillating wing.

2.1 Equations of Inviscid Flow

The equations of interest here are the 3D unsteady compressible Euler equations, expressed in a cartesian coordinate system $Ox_1x_2x_3$ in the conservation form

$$\frac{\partial \mathbf{U}}{\partial t} + \frac{\partial \mathbf{F}^j}{\partial x_j} = 0 \qquad j = 1,2,3 \tag{1}$$

where the sumation convention is employed and where

$$\mathbf{U} = \begin{bmatrix} \rho \\ \rho u_1 \\ \rho u_2 \\ \rho u_3 \\ \rho \epsilon \end{bmatrix} \tag{2}$$

is the unknown vector of conservation variables. The inviscid flux vectors are defined by

$$\mathbf{F}^j = \begin{bmatrix} \rho u_j \\ \rho u_1 u_j + p\delta_{1j} \\ \rho u_2 u_j + p\delta_{2j} \\ \rho u_3 u_j + p\delta_{3j} \\ (\rho \epsilon + p) u_j \end{bmatrix} \tag{3}$$

Here p, ρ and ϵ denote the pressure, density and specific total energy of the fluid respectively, while the component of the fluid velocity in the direction x_j is denoted by u_j. The equation set is completed by the addition of the perfect gas equation of state

$$p = (\gamma - 1)\rho(\epsilon - 0.5u_m^2) \tag{4}$$

where γ denotes the ratio of the specific heats.

For the purpose of deriving algorithms for the solution of these equations in a region Ω bounded by a closed surface Γ, using general unstructured tetrahedral grids, it is convenient to start from the alternative weak variational formulation: find $\mathbf{U}(\mathbf{x}, t)$ such that

$$\int_\Omega \frac{\partial \mathbf{U}}{\partial t} W d\Omega = \int_\Omega \mathbf{F}^j \frac{\partial W}{\partial x_j} d\Omega - \int_\Gamma \bar{\mathbf{F}}^{(n)} W d\Gamma \tag{5}$$

for every suitable weighting function $\mathrm{W}(\mathbf{x})$ and every $t > 0$, subject to $\mathbf{U}(\mathbf{x}, 0) = \mathbf{U}_0(\mathbf{x})$. In equation (5), the quantity $\bar{\mathbf{F}}^{(n)}$ is defined by

$$\bar{\mathbf{F}}^{(n)} = \mathbf{F}^j n^j \tag{6}$$

where $\mathbf{n} = (n_1, n_2, n_3)$ denotes the unit outward normal to Γ. The exact form of $\bar{\mathbf{F}}^{(n)}$ will depend on both the boundary condition being simulated and the local value of the solution.

2.2 Unstructured Grid Solution Algorithms

The domain Ω is discretised using linear tetrahedral elements. In the standard finite element approach, a piecewise linear approximate solution $\mathbf{U}^*$ is constructed in the form

$$\mathbf{U}^* = \mathbf{U}_J N_J(\mathbf{x}) \tag{7}$$

where $N_J(\mathbf{x})$ denotes the piecewise linear finite element shape function associated with node J of the grid and $\mathbf{U}_J = \mathbf{U}_J(t)$ denotes the value of the approximate solution at node J. The nodal values are obtained from a standard Galerkin method, which is based upon the weak formulation of the problem in which the approximation is constructed by employing the shape functions themselves as the weighting functions (Johnson,1987). Here, this is expressed as: find $\mathbf{U}^*$ such that

$$\int_\Omega \frac{\partial \mathbf{U}^*}{\partial t} N_I d\Omega = \int_\Omega \mathbf{F}^{j*} \frac{\partial N_I}{\partial x_j} d\Omega - \int_\Gamma \bar{\mathbf{F}}^{(n)} N_I d\Gamma \tag{8}$$

for every node I in the grid. The assumed form of $\mathbf{U}^*$ from equation (7) is inserted into this expression and the left hand side directly evaluated as

$$\int_\Omega \frac{\partial \mathbf{U}^*}{\partial t} N_I d\Omega = \mathbf{M}_{IJ} \frac{d\mathbf{U}_J}{dt} \tag{9}$$

where $\mathbf{M}_{IJ}$ denotes the entries in the standard consistent mass matrix. The right hand side terms in equation (8) are evaluated by making use of the local nature of the finite element shape functions. The process is illustrated here for the domain integral only. Suppose that each edge in the grid is numbered and that the information about the grid is given in terms of the nodes which are joined by these edges. Suppose also that edge S in the grid joins the interior node I with node S_1. If it is assumed that the fluxes are also linearly interpolated in terms of their nodal values i.e.

$$\mathbf{F}^{j*} \approx \mathbf{F}^j(\mathbf{U}_J) N_J(\mathbf{x}) = \mathbf{F}^j_J N_J(\mathbf{x}) \tag{10}$$

then it can be readily shown (Peraire, Peiró & Morgan 1993) that

$$\int_\Omega \mathbf{F}^{j*} \frac{\partial N_I}{\partial x_j} d\Omega = \sum_{S \in I} C^j_{I,S_1} \left(\mathbf{F}^j_I + \mathbf{F}^j_{S_1} \right) \tag{11}$$

where C^j_{I,S_1} denotes the weight that must be applied to the sum of the edge nodal fluxes in order to obtain the contribution made to node I by the edge which joins nodes I and S_1. With an edge based representation for the grid, the discretised equation at an interior node I can therefore be written as

$$\mathbf{M}_{IJ}\frac{d\mathbf{U}_J}{dt} = \sum_{S \varepsilon I} C^j_{I,S_1}\left(\mathbf{F}^j_I + \mathbf{F}^j_{S_1}\right) \tag{12}$$

It can be readily demonstrated from this expression that the flux at node I does not contribute to the discretised equation at node I, so that the application of the Galerkin method leads to a scheme which is central difference in character. In addition, the total contribution made by any interior edge in the grid is zero, so that the scheme can immediately be seen to be conservative in this sense.

To produce practical schemes for the simulation of compressible flows, we can employ the approach which is frequently adopted in 1D and replace the actual fluxes in equation (12) by appropriate consistent numerical fluxes. To achieve this in a convenient manner, we begin by defining the vector

$$\mathbf{C}_{I,S_1} = (C^1_{I,S_1}, C^2_{I,S_1}, C^3_{I,S_1}) \tag{13}$$

and the quantities

$$\mathcal{L}_{I,S_1} = |\mathbf{C}_{I,S_1}| \qquad \mathcal{S}^j_{I,S_1} = C^j_{I,S_1}/\mathcal{L}_{I,S_1} \tag{14}$$

Then, the equation at node I may be expressed as

$$\mathbf{M}_{IJ}\frac{d\mathbf{U}_J}{dt} = \sum_{S \varepsilon I} \mathcal{L}_{I,S_1}\Phi_{I,S_1} \tag{15}$$

where

$$\mathcal{F}_I = \mathbf{F}^j_I \mathcal{S}^j_{I,S_1} \qquad \mathcal{F}_{S_1} = \mathbf{F}^j_{S_1}\mathcal{S}^j_{I,S_1} \tag{16}$$

are the actual fluxes, in the direction of the vector $\mathbf{C}_{I,S_1}$, associated with the two nodes belonging to the edge S and

$$\Phi_{I,S_1} = (\mathcal{F}_I + \mathcal{F}_{S_1}) \tag{17}$$

denotes the actual flux associated with the edge S. Practical solution schemes for the compressible Euler equations on general unstructured meshes follow by replacing Φ by a consistent $\tilde{\Phi}$, which is constructed on the basis of 1D arguments.

Centered Schemes

Finite Element Lax-Wendroff Method

This is a simple finite element scheme for the solution of the compressible Euler equations on unstructured grids and is the finite element equivalent of the finite difference Lax-Wendroff method. For a problem involving only the spatial direction x_1, the Lax-Wendroff flux function is defined as (Hirsch 1990)

$$\tilde{\Phi} = \Phi - \frac{\Delta t}{2h_S}\mathbf{A}_S\left(\mathbf{F}^1_{S_1} - \mathbf{F}^1_I\right) \tag{18}$$

where Δt is a time step, $\mathbf{A}_S = d\mathbf{F}^1/d\mathbf{U}$ is the Jacobian matrix of $\mathbf{F}^1$ and h_S is the length of the edge S. By direct extension to the multi-dimensional case, a Lax-Wendroff type scheme, for general tetrahedral grids, is written in the form

$$\mathbf{M}_{IJ}\Delta\mathbf{U}_J = \Delta t \sum_{S \varepsilon I} \mathcal{L}_{I,S_1}\tilde{\Phi}^n_{I,S_1} \tag{19}$$

where

$$\tilde{\Phi} = \Phi - \frac{\Delta t}{2h_S}\mathbf{A}_S\left(\mathcal{F}_{S_1} - \mathcal{F}_I\right) \tag{20}$$

In equation (19),

$$\Delta\mathbf{U} = \mathbf{U}^{n+1} - \mathbf{U}^n \tag{21}$$

the superscript n denotes the time level, $\Delta t = t_{n+1} - t_n$ and $\mathbf{A}_S = d\mathcal{F}/d\mathbf{U}$. For the simulation of transient problems, one possible approach is to solve equation (19) by explicit iteration (Morgan & Peraire 1987), though this will prove to be an expensive procedure in general. For steady flow simulations, the consistent mass matrix $\mathbf{M}$ is replaced by the diagonal lumped mass matrix $\mathbf{M_L}$ to produce a truly explicit scheme.

A Multi-Stage Method

An approach which has proved to be extremely successful for the simulation of compressible transonic Euler flows is the use of a central difference discretisation in space together with the explicit addition of a stabilising scalar high order added artificial viscosity (Jameson 1987). For a problem involving only the spatial direction x_1, a suitable flux function for a scheme of this form is

$$\tilde{\Phi}_{I,S_1} = \Phi_{I,S_1} - d_4 \left| \lambda_S \right| \left[\mathbf{U}_{S_1} - \mathbf{U}_S - \left(h_S \frac{d\mathbf{U}^*}{d\eta} \right)_S \right] \tag{22}$$

where the coordinate η runs along the edge from node I to node S_1. In equation (22), d_4 denotes a user-specified constant and $\left| \lambda \right|$ is the maximum eigenvalue, in absolute value, of the Jacobian matrix $\mathbf{A}_S$. To implement this procedure, nodal gradients are calculated, using equation (11), in the form

$$[\mathbf{M_L}]_{II} \left. \frac{\partial \mathbf{U}^*}{\partial x_j} \right|_I = - \sum_{S \in I} C^j_{I,S_1} (\mathbf{U}_I + \mathbf{U}_{S_1}) \tag{23}$$

with $j = 1$. The required edge gradients are obtained as the average of the edge nodal gradients. Expression (22) for the flux function can be shown to possess the property that the diffusion which is added is zero, on any grid, whenever $\mathbf{U}^*$ is linear. By direct extension, we employ the flux function of equation (22) directly for the multi-dimensional case on general tetrahedral grids.

The resulting equation can be advanced in time via the explicit multi-stage time stepping scheme

$$\begin{aligned} \mathbf{U}_I^{(0)} &= \mathbf{U}_I^n \\ \mathbf{U}_I^{(k)} &= \mathbf{U}_I^n + \alpha_k \Delta t \, [\mathbf{M_L}]^{-1}_{II} \sum_{S \in I} \mathcal{L}_{I,S_1} \tilde{\Phi}^{(k-1)}_{I,S_1} \quad k = 1, \ldots, m \\ \mathbf{U}_I^{n+1} &= \mathbf{U}_I^{(m)} \end{aligned} \tag{24}$$

In an alterative implementation (Swanson & Turkel 1990), the scalar diffusion coefficient, $\left| \lambda_S \right|$, in equation (22) is replaced by a matrix coefficient, leading to the numerical flux function

$$\tilde{\Phi}_{I,S_1} = \Phi_{I,S_1} - d_4 \left| \mathbf{A}_S (\mathbf{U}_I, \mathbf{U}_{S_1}) \right| \left[\mathbf{U}_{S_1} - \mathbf{U}_S - \left(h_S \frac{d\mathbf{U}^*}{d\eta} \right)_S \right] \tag{25}$$

where $\left| \mathbf{A}_S (\mathbf{U}_I, \mathbf{U}_{S_1}) \right|$ denotes the standard Roe matrix (Roe 1981) evaluated in the direction $\mathbf{C}_{I,S_1}$.

Shock Capturing

Additional explicitly added low order artificial viscosity is needed if either of the above schemes is to be used successfully for the simulation of flows containing discontinuities. By comparison with the one dimensional case, it is apparent that the addition of diffusion in the multi-dimensional situation can be simply achieved by the use of the flux function

$$\bar{\tilde{\Phi}}_{I,S_1} = \tilde{\Phi}_{I,S_1} - d_2 \pi_S \left| \lambda_S \right| [\mathbf{U}_{S_1} - \mathbf{U}_I] \tag{26}$$

where d_2 is a user defined constant. To maintain the accuracy of the original schemes in the smooth regions of the flow, an edge pressure switch π_S has been built into the definition of this additional diffusion. This pressure switch is designed to be significant only near any flow discontinuities and to be very small in the smooth flow regions (Peraire, Morgan, Peiró & Zienkiewicz 1987). The alternative expression

$$\bar{\tilde{\Phi}}_{I,S_1} = \tilde{\Phi}_{I,S_1} - d_2 \pi_S \left| \mathbf{A}_S (\mathbf{U}_I, \mathbf{U}_{S_1}) \right| [\mathbf{U}_{S_1} - \mathbf{U}_I] \tag{27}$$

in which the scalar diffusion coefficient in equation (26) is replaced by a matrix diffusion coefficient, may also be employed here.

Higher Resolution via Flux Corrected Transport

Flux corrected transport (FCT) is a technique introduced originally (Boris & Book 1973, Zalesak 1979) to produce high resolution monotone solutions by combining the results of a low order monotone scheme with those of a higher order scheme. Unstructured grid implementations have proved successful (Parrott & Christie 1986, Morgan, Peraire & Löhner 1988), particularly for transient simulations. The approach only needs slight modification for implementation in the curent context. For example, for the Lax-Wendroff type scheme, let $\Delta \mathbf{U}^H$ be the basic (high order) solution increment and let $\Delta \mathbf{U}^L$ be the (low order) increment computed with the same algorithm but with the addition of the unswitched (i.e. $\pi_S = 1$) shock capturing diffusion of equation (26). If this added diffusion is denoted by $\mathbf{D}$, it follows that these increments are related by

$$\Delta \mathbf{U}^H = \Delta \mathbf{U}^L - \mathbf{D} \tag{28}$$

It is apparent from equation (26) that the diffusion $\mathbf{D}$ is formed as the sum of edge contributions i.e.

$$\mathbf{D} = \sum_{S \epsilon I} \mathbf{D}_{I,S_1} \tag{29}$$

The idea behind FCT is to limit the amount of artificial diffusion which is removed from the low order solution to produce the high order solution in equation (28) by imposing the requirement that the high order solution should remain monotone. This is achieved by firstly identifying maximum and minimum allowable values for the solution at node I. We define

$$\mathbf{U}^H = \mathbf{U}^n + \Delta \mathbf{U}^H \qquad \mathbf{U}^L = \mathbf{U}^n + \Delta \mathbf{U}^L \tag{30}$$

and the maximum and minimum allowable nodal values are determined as

$$\begin{aligned} \mathbf{U}_I^{max} &= \max_{S \epsilon I} \left(\mathbf{U}_I^L, \mathbf{U}_{S_1}^L, \mathbf{U}_I^n, \mathbf{U}_{S_1}^n \right) \\ \mathbf{U}_I^{min} &= \min_{S \epsilon I} \left(\mathbf{U}_I^L, \mathbf{U}_{S_1}^L, \mathbf{U}_I^n, \mathbf{U}_{S_1}^n \right) \end{aligned} \tag{31}$$

Edge limiters ψ_S are determined so as to ensure that the increment computed according to

$$\Delta \mathbf{U} = \Delta \mathbf{U}^L - \sum_{S \epsilon I} \psi_S \mathbf{D}_{I,S_1} \tag{32}$$

is such that the new solution at each node lies within the range specified by these maximum and minimum values. In practice, the edge limiter is determined from the requirement that variables such as density, pressure and Mach number should remain monotone. As well as producing high resolution solutions, the FCT procedure acts as a stabilising influence on centered schemes when they are applied in the hypersonic range. Thus, with the addition of FCT, the explicit multi-stage time stepping scheme has been employed to solve the problem of steady flow over a space shuttle type configuration at a Mach number of ten and at thirty degrees angle of attack. A view of the surface grid used in the simulation is shown in Figure 1a and the computed distribution of the Mach number contours can be seen in Figure 1b. The complete unstructured grid, for one half of the configuration, consisted of 1,462,189 elements and 269,780 nodes.

Upwind Methods

By similar direct extension of schemes developed for the solution of the compressible Euler equations in 1D, a first order upwind method for general unstructured grids can be constructed by the use of the flux function

$$\tilde{\mathbf{\Phi}}_{I,S_1} = \mathbf{\Phi}_{I,S_1} - \left| \mathbf{A}_S \left(\mathbf{U}_I, \mathbf{U}_{S_1} \right) \right| \left[\mathbf{U}_{S_1} - \mathbf{U}_I \right] \tag{33}$$

Higher order methods can be derived by employing MUSCL (van Leer 1979) or TVD concepts (Harten 1983, 1984).

In the MUSCL scheme (Vahdati, Morgan & Peraire 1992), the gradient of the solution is computed at the nodes, as in equation (23), and the solution is linearly reconstructed for each edge. Slope limiting is applied to ensure that the reconstructed solution does not go above (below) the maximum (minimum) of the value of the solution at the nodes of all elements associated with the two nodes of the edge. With a reconstructed solution, the scheme employs the numerical flux function

$$\tilde{\Phi}_{I,S_1} = (\mathcal{F}_I^+ + \mathcal{F}_{S_1}^-) - \left| \mathbf{A}_S \left(\mathbf{U}_I^+, \mathbf{U}_{S_1}^- \right) \right| \left[\mathbf{U}_{S_1}^- - \mathbf{U}_I^+ \right] \tag{34}$$

where the superscripts + and − denote mid–edge states, which are determined from the reconstructed solution.

In a TVD implementation (Lyra, Morgan, Peraire and Peiró 1993), points S_2 and S_3 are located in the grid such that (a) S_2 and S_3 lie on the line of the edge S (b) S_2 and S_1 are equidistant from I (c) S_2 lies on the opposite side of the point I to the point S_1 (d) I and S_3 are equidistant from S_1 (c) S_3 lies on the opposite side of the point S_1 to the point I. The TVD flux is computed as (Yee 1989)

$$\tilde{\Phi}_{I,S_1} = \Phi_{I,S_1} - \mathbf{R}^{-1} \left| \Lambda \right| \mathbf{Q} \tag{35}$$

where the Roe matrix is decomposed according to

$$\left| \mathbf{A}_S \right| = \mathbf{R}^{-1} \left| \Lambda \right| \mathbf{R} \tag{36}$$

In this expression $\mathbf{R}$ denotes the matrix whose columns are the right eigenvectors of the Roe matrix and $\left| \Lambda \right|$ is the diagonal matrix whose entries are the absolute values of the eigenvalues of $\mathbf{A}_S$. In equation (35),

$$\mathbf{Q} = \psi_{I,S_1} - \text{minmod} \left(\psi_{S_2,I}, \psi_{I,S_1}, \psi_{S_1,S_3} \right) \tag{37}$$

where

$$\psi_{I,S_1} = \mathbf{R} (\mathbf{U}_{S_1} - \mathbf{U}_I) \tag{38}$$

With either of these schemes, the solution can be advanced in time to steady state by any suitable time stepping procedure.

Grid Data Structure

For a general 3D grid of linear tetrahedral elements, the number of elements is approximately 5.5 times the number of nodes, the number of triangular faces is approximately twice the number of elements and the number of edges is approximately equal to the number of elements plus the number of nodes. Using these relations, it is possible to show that, in addition to being useful for the creation of flow algorithms, the adoption of the edge based representation for the unstructured grid has important computational implications. This is illustrated in the table below, which compares the storage and cpu requirements for an explicit

Data Structure	Storage/Node	cpu/node
Element	25*	1.0*
	71.5	0.88
Face	58*	1.4*
	88	1.2
Edge	32.5	0.6

*With recomputation of the geometry

centered unstructured grid solution algorithm for the solution of the compressible Euler equations. The grid data structures which are considered in this table are the traditional finite element data structure, the face data structure, which is frequently favoured by the developers of finite volume algorithms, and the edge data structure, which has been considered in detail above. It can be observed that the computer code based

upon the edge data structure for the grid is the most efficient in terms of cpu requirements and is close to being optimal in terms of its storage demands.

2.3 Convergence Acceleration

The solution of complex steady 3D flows on unstructured grids is most commonly achieved by explicit time stepping. Although this approach is robust, it can prove expensive in terms of cpu requirements, as a large number of time steps is frequently needed to produce a converged solution. There is therefore the requirement to search for more effective solution approaches, especially with the perceived increasing industrial demand for the development of a capability for the solution of large scale viscous flow problems.

Multigrid Methods

Multigrid acceleration coupled with an explicit multi-stage time stepping scheme has proved to be an extremely effective method for the solution of the compressible Euler equations on structured grids (Jameson 1983). The basic idea of the multigrid method is to use the residuals computed on a given grid to drive a time marching scheme on a coarse grid. The corrections to the unknowns computed on the coarser grid are then added to the fine grid solution. The time marching scheme on the coarse grid may itself be accelerated by the use of an even coarser grid and, in this way, the multigrid concept can be extended to incorporated any number of coarse grids. Advancing the solution on the coarse grids is computationally relatively inexpensive, because of the reduced number of unknowns and the larger allowable time step size. The necessary intergrid transfers are readily accomplished because of the nested nature of the grid sequence.

The development of appropriate intergrid transfer operators is a complication that has to be addressed when attempting to implement a similar multigrid acceleration scheme within the unstructured grid environment (Mavriplis 1988, Mavriplis 1991, Peraire, Morgan and Peiró 1993).

2.4 Transient Problems

Although the time dependent form of the equations has been employed, the main thrust of the arguments presented above has been directed at the simulation of steady flows, where the solution is obtained via a false transient. The extension of these techniques to the simulation of truly time dependent flows is now considered. The particular problem of simulating the flow over an oscillating wing has been chosen as an illustrative example.

Flow Over an Oscillating Wing

Two dimensional simulations of transonic inviscid flows over oscillating bodies have been performed using the full range of techniques currently available to the unstructured grid researcher. To allow for the movement of the boundary and the transient development of the solution, adaptive remeshing can be utilised. To improve the efficiency of the explicit computational procedure, on meshes exhibiting large variations in element size, a domain decomposition technique can be included. In the domain decomposition method, different time steps are employed in different areas of the grid, while maintaining the time accuracy of the overall solution procedure. Typical results are shown in Figures 2 and 3 for a standard AGARD test case involving flow at a freestream Mach number of 0.755 over an oscillating NACA0012 aerofoil. The procedure can also be used in a predictive mode, as shown in Figure 4 which displays the results of the flow over a NACA0012 aerofoil in which the rear portion only of the aerofoil is oscillating.

Such comprehensive 2D computations place large demands on current computational resources. For 3D simulations, we therefore decided to investigate if we could produce an approach which is more in line with the current computational resources, at the expense of a certain degree of generality. To achieve this, we restricted consideration to simulations in which a moving boundary would actually be simulated by keeping the boundary and the mesh fixed and then applying a suitably modified boundary condition. This avoids the necessity of expensive remeshing procedures to allow for the boundary motion. To produce a further improvement in the computational performance, the explicit timestepping scheme is replaced by an implicit procedure. This allows for the adoption of larger timesteps, while still maintaining sufficient time accuracy. The solution of an implicit equation system resulting from the 3D Euler equations is a non-trivial task and the approach followed here has been to achieve this by the application of the multigrid method.

Approximation to the Wing Boundary Condition

To be able to impose the boundary condition at any point on a moving solid surface, we need to know the normal vector $\mathbf{n}$ to the surface and the normal velocity $\mathbf{v}_n$ of the surface at the point. The surface boundary

condition is then imposed by replacing the computed fluid velocity $\mathcal{V}$ by $\mathcal{V}^*$ according to

$$\mathcal{V}^* = \underbrace{\mathcal{V} - (\mathcal{V} \cdot \mathbf{n})\,\mathbf{n}}_{\text{tangential}} + \underbrace{\mathbf{v}_n}_{\text{normal}} \tag{39}$$

The intention here is to keep the boundary fixed and to simulate its actual motion through a boundary condition of the form of equation (39). Suppose the angle of attack, α, of the wing is actually changing in time according to

$$\alpha = \alpha_0 \sin(\omega t + \phi) \tag{40}$$

The normal vector $\mathbf{n}$ at time t is computed from the original normal, $\mathbf{n}_0$, at time $t = 0$ as

$$\mathbf{n} = \mathcal{T}(\alpha)\mathbf{n}_0 \tag{41}$$

where $\mathcal{T}(\alpha)$ is a standard rotation matrix. The normal velocity of the wing surface is calculated from the total velocity $\mathcal{V}_T$ as

$$\mathbf{v}_n = \mathcal{V}_T \cdot \mathbf{n} \tag{42}$$

with the total velocity $\mathcal{V}_T$ determined as

$$\mathcal{V}_T = \mathbf{r} \times \frac{d\alpha}{dt} \tag{43}$$

where $\mathbf{r}$ denotes the position vector from the line of rotation to the point on the surface in question.

To investigate the usefulness of this form of the boundary condition, an initial investigation was undertaken in which a wing at an angle of attack was simulated (a) by inclining the flow direction and applying the standard inviscid boundary condition and (b) by a wing at zero angle of attack and applying the boundary condition of equations (39–43). The results show that the two approaches produce very similar results for reasonable angles of attack. For example, in Figure 5, we compare the pressure distributions, computed by the two approaches, over a section of an ONERA M6 wing for an angle of attack of four degrees. Results of this form give us confidence that the proposed approach can be used to give meaningful results for transient simulations in which the variation in the angle of attack is of this order.

An Implicit Timestepping Scheme

The spatial discretisation methods for the Euler equations which have been considered above lead to a discretised equation system

$$\frac{d\mathbf{U}}{dt} = \mathbf{R}(\mathbf{U}) \tag{44}$$

In the present context, we propose the use of an implicit three–level scheme in time (Jameson 1992) which can be expressed as

$$\frac{3\,\mathbf{U}^{n+1} - 4\,\mathbf{U}^n + \mathbf{U}^{n-1}}{2\,\Delta t} = \mathbf{R}(\mathbf{U}^{n+1}) \tag{45}$$

to advance the solution. Equation (45) can be re–arranged and written in the form

$$\mathbf{0} = \mathbf{R}^*(\mathbf{U}^{n+1}) + \mathbf{S}(\mathbf{U}^n, \mathbf{U}^{n-1}) \tag{46}$$

where

$$\mathbf{R}^*(\mathbf{U}^{n+1}) = \mathbf{R}(\mathbf{U}^{n+1}) - \frac{3}{2\,\Delta t}\mathbf{U}^{n+1} \tag{47}$$

and

$$\mathbf{S}(\mathbf{U}^n, \mathbf{U}^{n-1}) = \frac{2\,\mathbf{U}^n}{\Delta t} - \frac{\mathbf{U}^{n-1}}{2\Delta t} \tag{48}$$

Equation (46) can now be solved by using an explicit multi–stage time stepping scheme to obtain the steady state solution of the equation

$$\frac{d\mathbf{U}^{n+1}}{dt} = \mathbf{R}^*(\mathbf{U}^{n+1}) + \mathbf{S}(\mathbf{U}^n, \mathbf{U}^{n-1}) \tag{49}$$

with multigrid acceleration again employed to accelerate the convergence of the explicit time stepping.

The numerical performance of the proposed procedure is demonstrated by considering the transient development of the flow over an oscillating ONERA M6 wing. In the computation, the wing is held fixed and its sinusoidal oscillation is simulated by modifying the boundary condition at the wing surface, according to equations (39–43). As we have indicated previously, this approach can be expected to be valid for oscillations of small amplitude. Here the simulation involved an amplitude of four degrees and 40 multigrid cycles were used per timestep with 24 timesteps taken per cycle. A sequence of five meshes was employed in the multigrid procedure, with the form of the surface discretisations employed being indicated in Figure 6. The distribution of the pressure on the upper surface of the wing during the initial portion of the cycle is shown in Figure 7. The distribution of the pressure on the lower surface of the wing during the remainder of the cycle is shown in Figure 8.

3. CONCLUSIONS

A description of the research work undertaken under NASA Research Grant NAGW-2962 has been given. Basic algorithmic development work, undertaken for the simulation of steady 3D inviscid flows, has been used as the basis for the construction of a procedure for the simulation of truly transient flows in 3D. To produce a viable procedure for implementation on the current generation of computers, moving boundary components are simulated by fixed boundaries plus a suitably modified boundary condition. Computational efficiency is increased by the use of an implicit timestepping scheme in which the equation system is solved by explicit multistage timestepping with multigrid acceleration. The viablity of the proposed approach has been demonstrated by considering the application of the procedure to simulation of a transonic flow over an oscillating ONERA M6 wing.

REFERENCES

J.P. Boris and D.L. Book. 1973. Flux Corrected Transport I: SHASTA, A Fluid Transport Algorithm that Works. *Journal of Computational Physics* 11, 38–69.

A. Harten. 1983. High Resolution Schemes for Hyperbolic Conservation Laws. *Journal of Computational Physics* 49, 357–393.

A. Harten. 1984. On a Class of High Resolution Total Variation Stable Finite Difference Schemes. *SIAM Journal of Numerical Analysis* 21, 1–23.

C. Hirsch. 1990. *Numerical Computation of Internal and External Flows.* Wiley.

A. Jameson. 1983. Solution of the Euler Equations for Two Dimensional Transonic Flow by a Multigrid Method. *Applied Mathematics and Computation*, 13, 327–355.

A. Jameson. 1987. Successes and Challenges in Computational Aerodynamics. *AIAA Paper*, 87–1184.

A. Jameson. 1992. Time Dependent Calculations Using Multigrid, with Applications to Unsteady Flows Past Aerofoils and Wings. *AIAA Paper 91-1596*, 1991.

C. Johnson. 1987. *Numerical Solution of Partial Differential Equations by the Finite Element Method.* Cambridge University Press.

P.R.M. Lyra, K. Morgan, J. Peraire and J. Peiró. 1993. Unstructured Grid FEM/TVD Algorithm for Systems of Hyperbolic Conservation Laws. In: *Proceedings of the Conference on Numerical Methods for Laminar and Turbulent Flow, Edited by C. Taylor et al*, Pineridge Press, 1408–1420, 1993.

D. Mavriplis. 1988. Multigrid Solution of the Two Dimensional Euler Equations on Unstructured Triangular Meshes. *AIAA Journal* 26, 824–831.

D. Mavriplis. 1991. Three Dimensional Unstructured Multigrid for the Euler Equations. *AIAA Paper*, 91–1549.

K. Morgan and J. Peraire. 1987. Finite Element Methods for Compressible Flows. In: *von Karman Institute for Fluid Dynamics Lecture Series 1987-04*, Brussels, 1–114.

K. Morgan, J. Peraire and R. Löhner. 1988. Adaptive Finite Element Flux Corrected Transport Techniques for CFD. In: *Finite Elements—Theory and Applications, Edited by D.L. Dwoyer, M.Y. Hussaini and R.G. Voigt*, Springer–Verlag, 165–175.

A.K. Parrott and M.A. Christie. 1986. FCT Applied to the 2–D Finite Element Solution of Tracer Transport by Single Phase Flow in a Porous Medium. In: *Numerical Methods for Fluid Dynamics II, Edited by K.W. Morton and M.J. Baines*, Clarendon Press, 609–619.

J. Peraire, K. Morgan and J. Peiró. 1993. Multigrid Solution of the 3D Compressible Euler Equations on Unstructured Tetrahedral Grids. *International Journal for Numerical Methods in Engineering* 36, 1029–1044.
J. Peraire, K. Morgan, J. Peiró and O.C. Zienkiewicz. 1987. An Adaptive Finite Element Method for High Speed Flows. *AIAA Paper*, 87–0559.
J. Peraire, J. Peiró and K. Morgan. 1993. Finite Element Multigrid Solution of Euler Flows Past Installed Aero–Engines. *Computational Mechanics* 11, 433–451.
P. Roe. 1981. Approximate Riemann Solvers. Parameter Vectors and Difference Schemes. *Journal of Computational Physics* 43, 357–372.
V. Shankar, W.F. Hall, A. Mohammadian and C. Rowell. 1993. Algorithmic Aspects and Trends in Computational Electromagnetics. *AIAA Paper*, 93–0367.
R.C. Swanson and E. Turkel. 1990. On Central Difference and Upwind Schemes. *ICASE Report*, 90–44.
M. Vahdati, K. Morgan and J. Peraire. 1992. Computation of Viscous Compressible Flows Using an Upwind Algorithm and Unstructured Meshes. In: *Computational Mechanics in Aerospace Engineering. Edited by S.N. Atluri*, AIAA Progress in Astronautics and Aeronautics Series Volume 146, 479–505.
B. van Leer. 1979. Towards the Ultimate Conservative Difference Scheme. V. A Second Order Sequel to Godunov's Method. *Journal of Computational Physics* 32, 101–136.
H.C. Yee. 1989. A Class of High–Resolution Explicit and Implicit Shock–Capturing Methods. In: *von Karman Institute for Fluid Dynamics Lecture Series 1989–04*, Brussels, 1–216.
S.T. Zalesak. 1979. Fully Multidimensional Flux Corrected Transport Algorithms for Fluids. *Journal of Computational Physics* 31, 335–362.

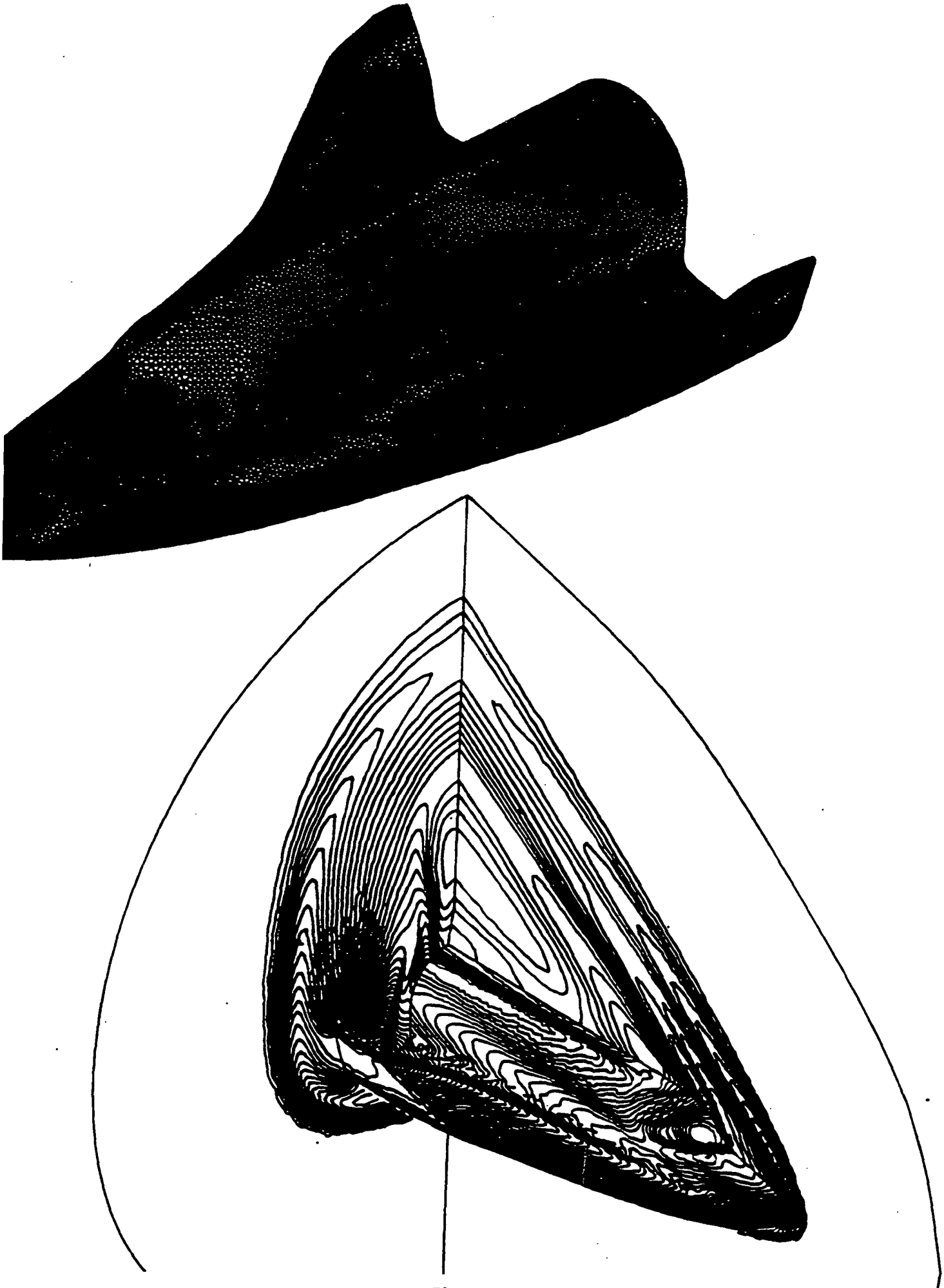

Figure 1

The simulation of steady hypersonic inviscid flow over a space shuttle configuration. Free stream Mach number = 10; angle of attack = 30 degrees. (a) View of the surface triangulation. (b) Computed distribution of Mach number contours.

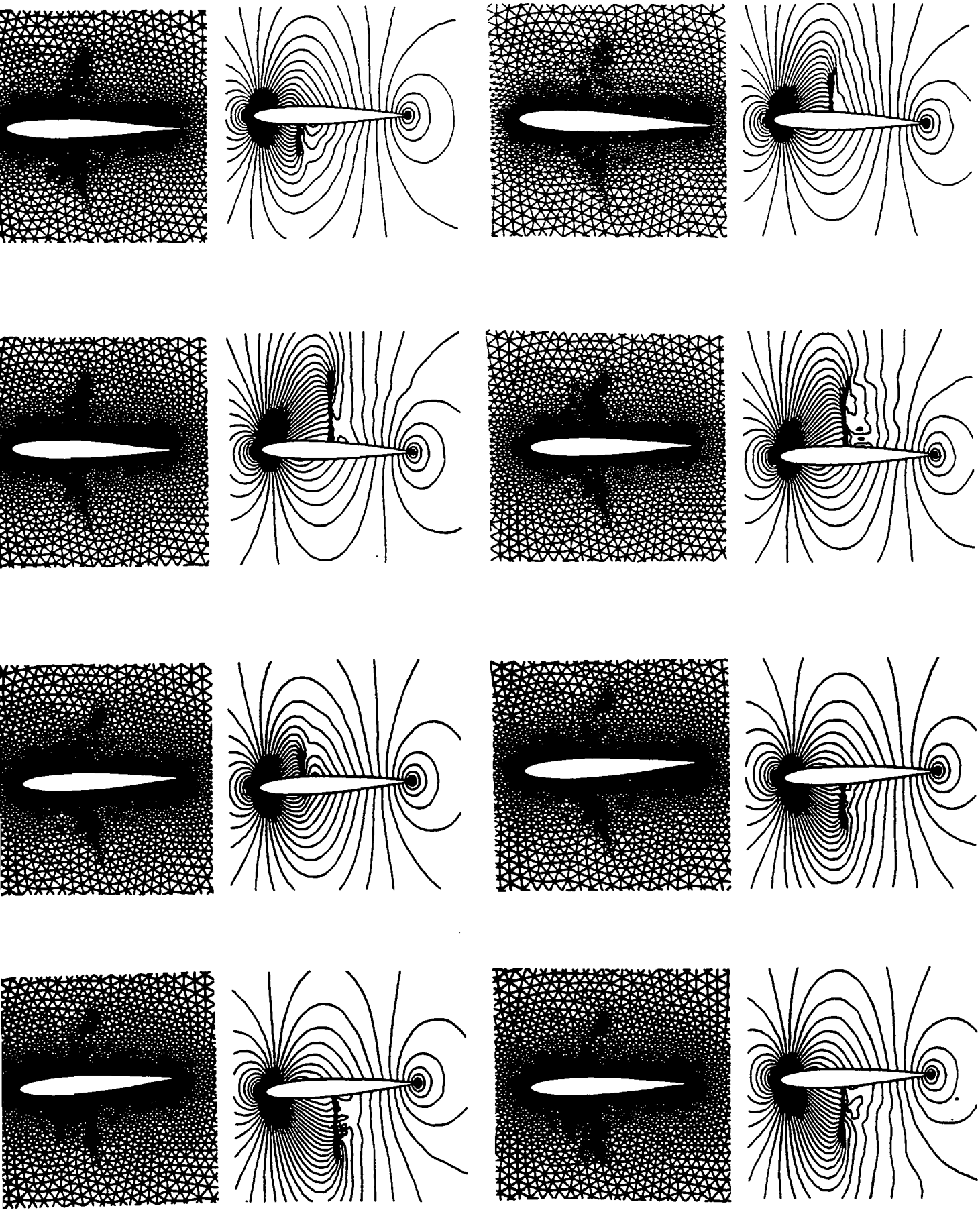

Figure 2

The simulation of inviscid flow over an oscillating NACA0012. Free stream Mach number = 0.755. Details of the adapted meshes and computed pressure coefficient contours at different stages of the cycle.

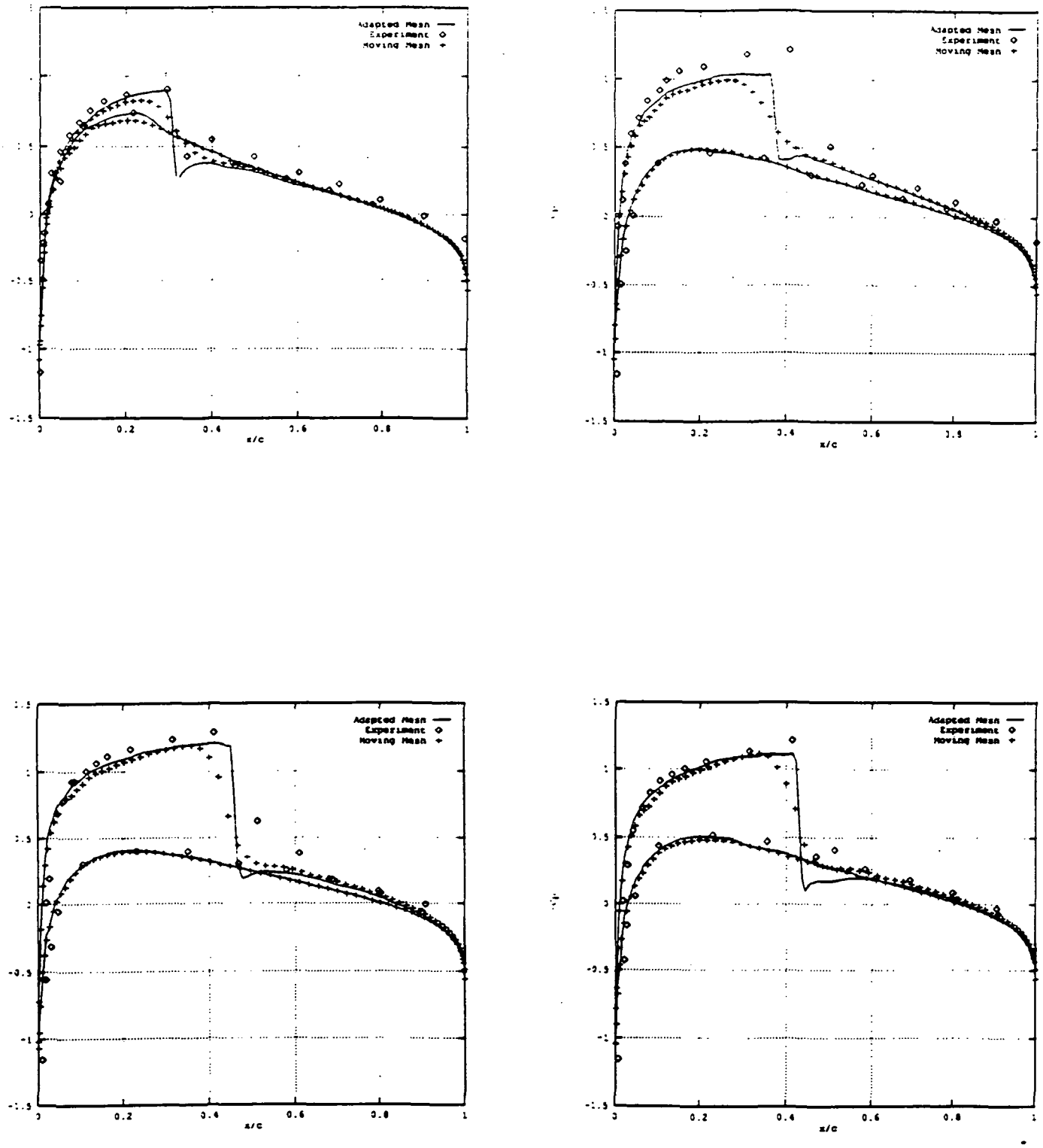

Figure 3

The simulation of inviscid flow over an oscillating NACA0012. Free stream Mach number = 0.755. Distribution of the computed pressure coefficient over the aerofoil surface showing a comparison with experiment and with the results of a simulation in which the mesh was adapted by moving only.

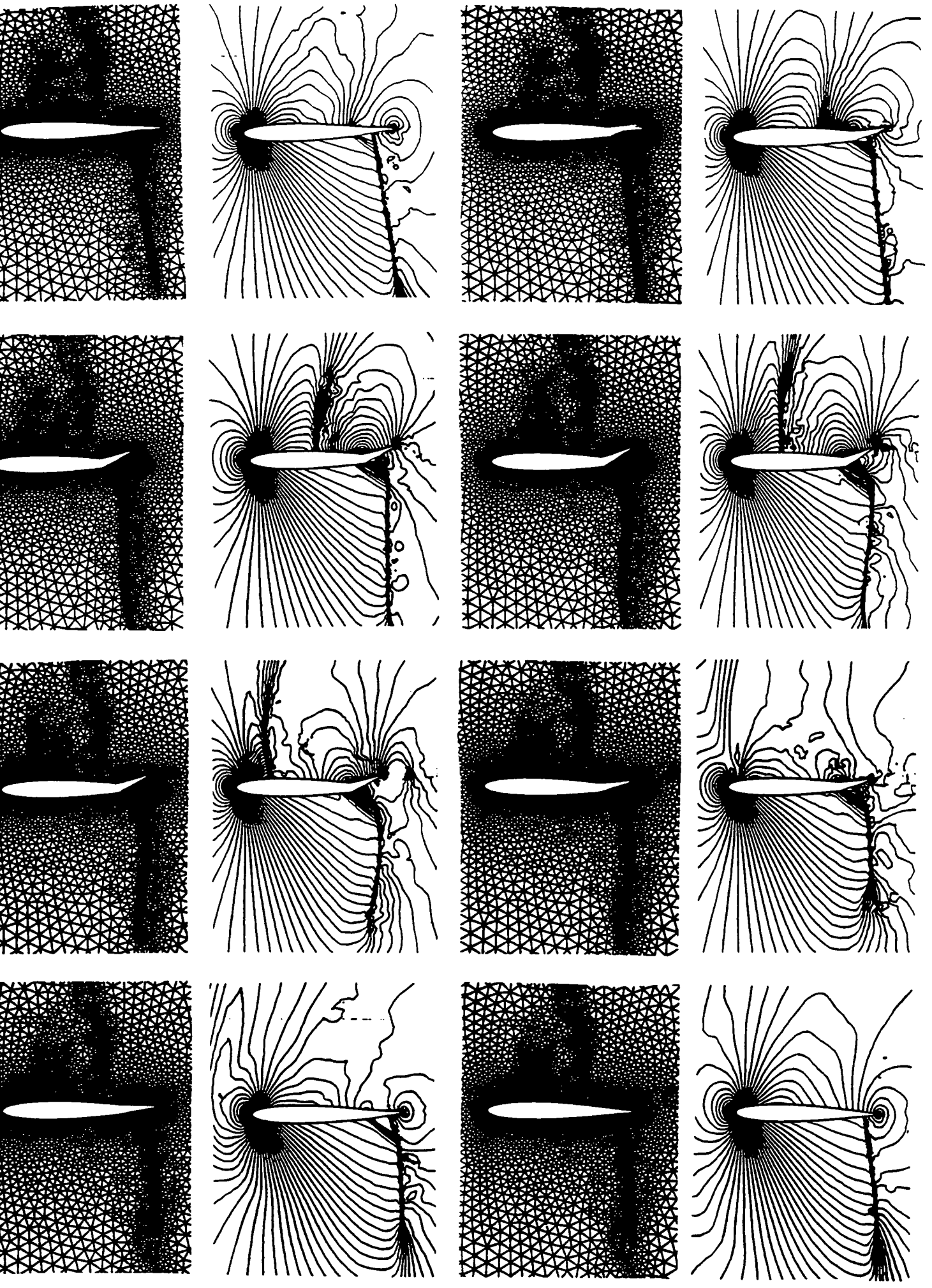

Figure 4

The simulation of inviscid flow over a NACA0012, with the rear portion of the aerofoil oscillating sinusoidally.. Free stream Mach number = 0.8. Details of the adapted meshes and computed pressure coefficient contours at different stages of the cycle.

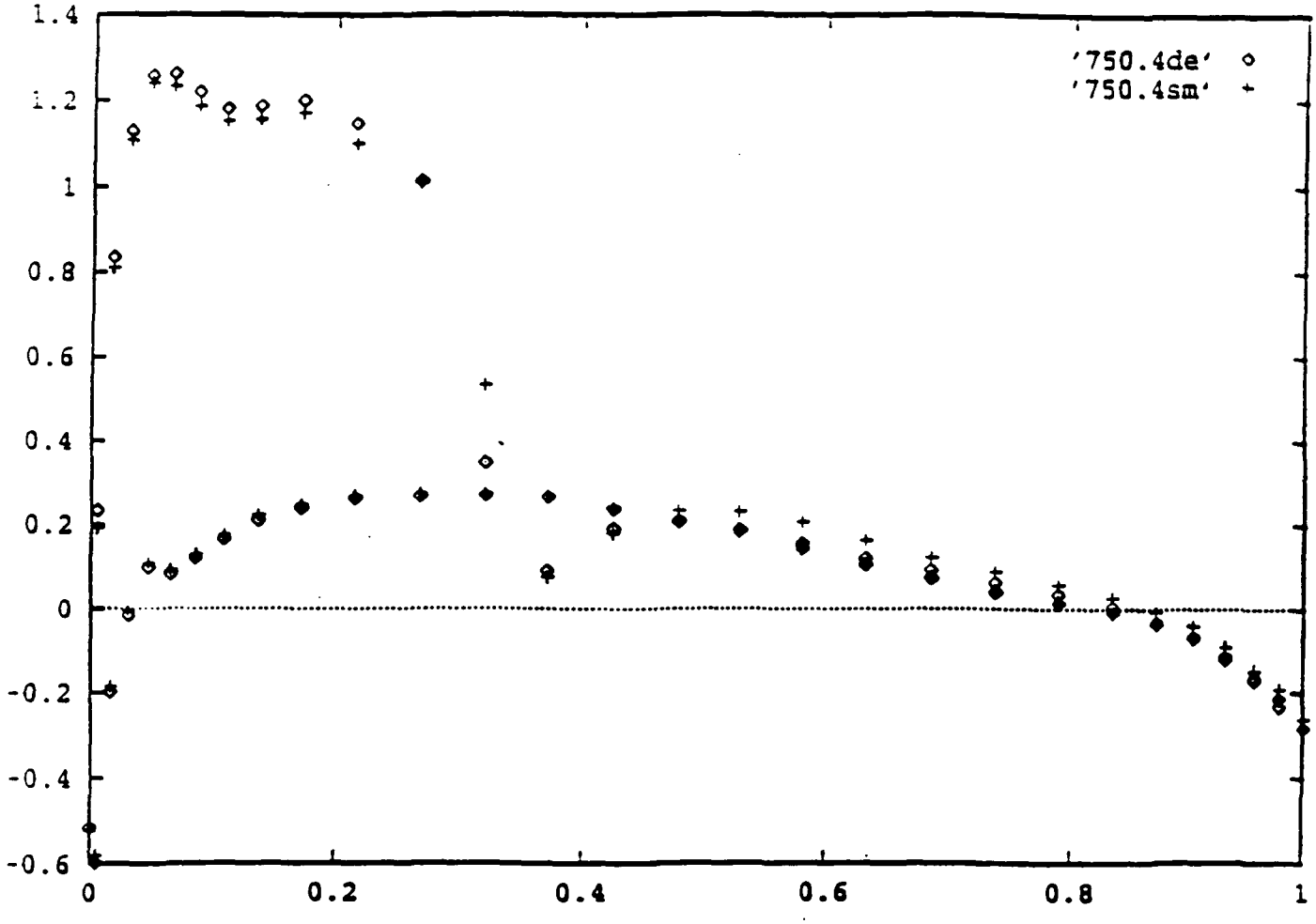

Figure 5

The simulation of inviscid transonic flow over an ONERA M6 wing at 4 degrees angle of attack. Comparison of the computed pressure distributions over a section obtained using an inclined stream (de) and the modified boundary condition (sm).

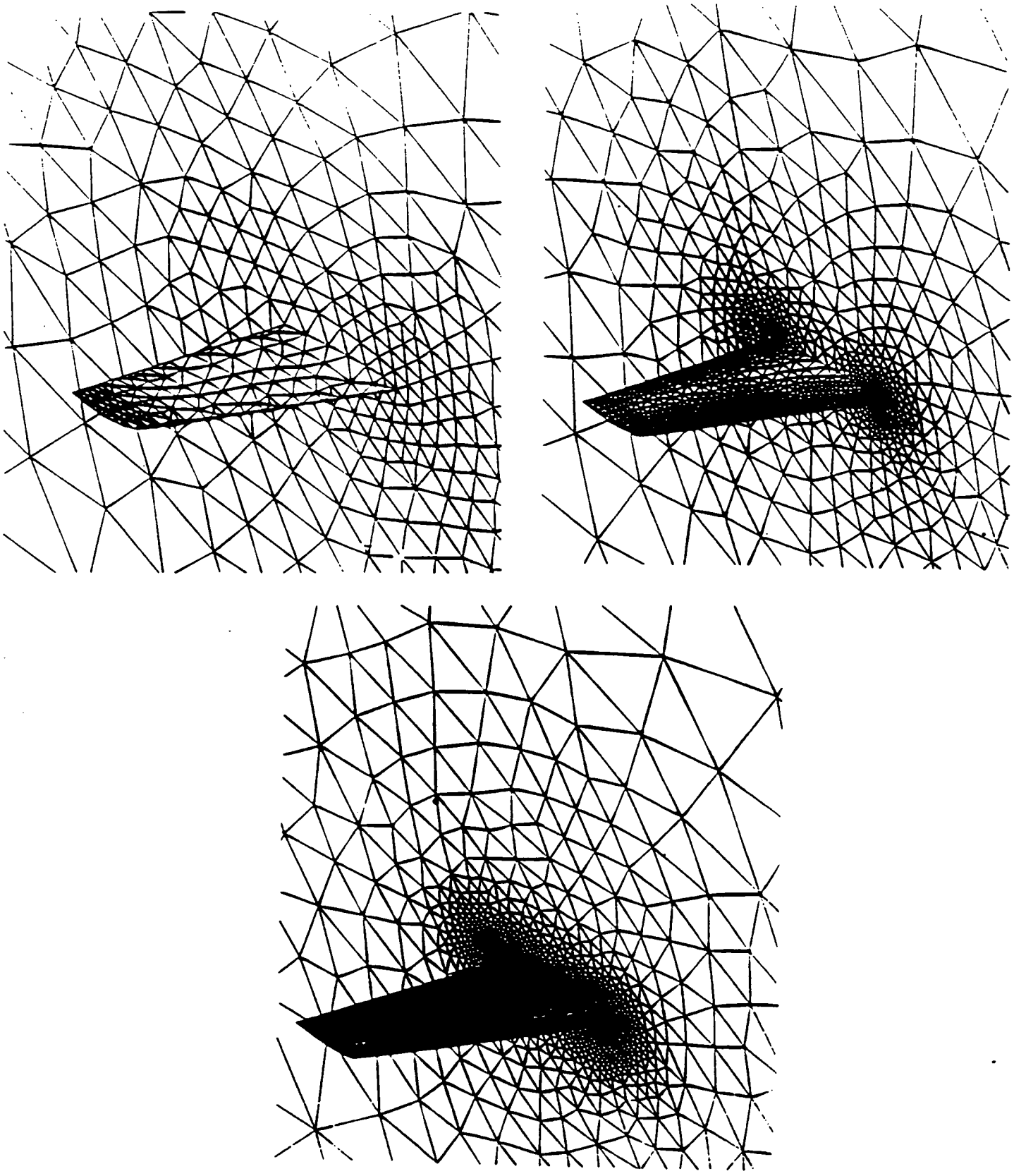

Figure 6

The simulation of inviscid transonic flow over a sinusoidally oscillating ONERA M6 wing. The surface discretisation on (a) The finest grid. (b) An intermediate grid. (c) The coarsest grid.

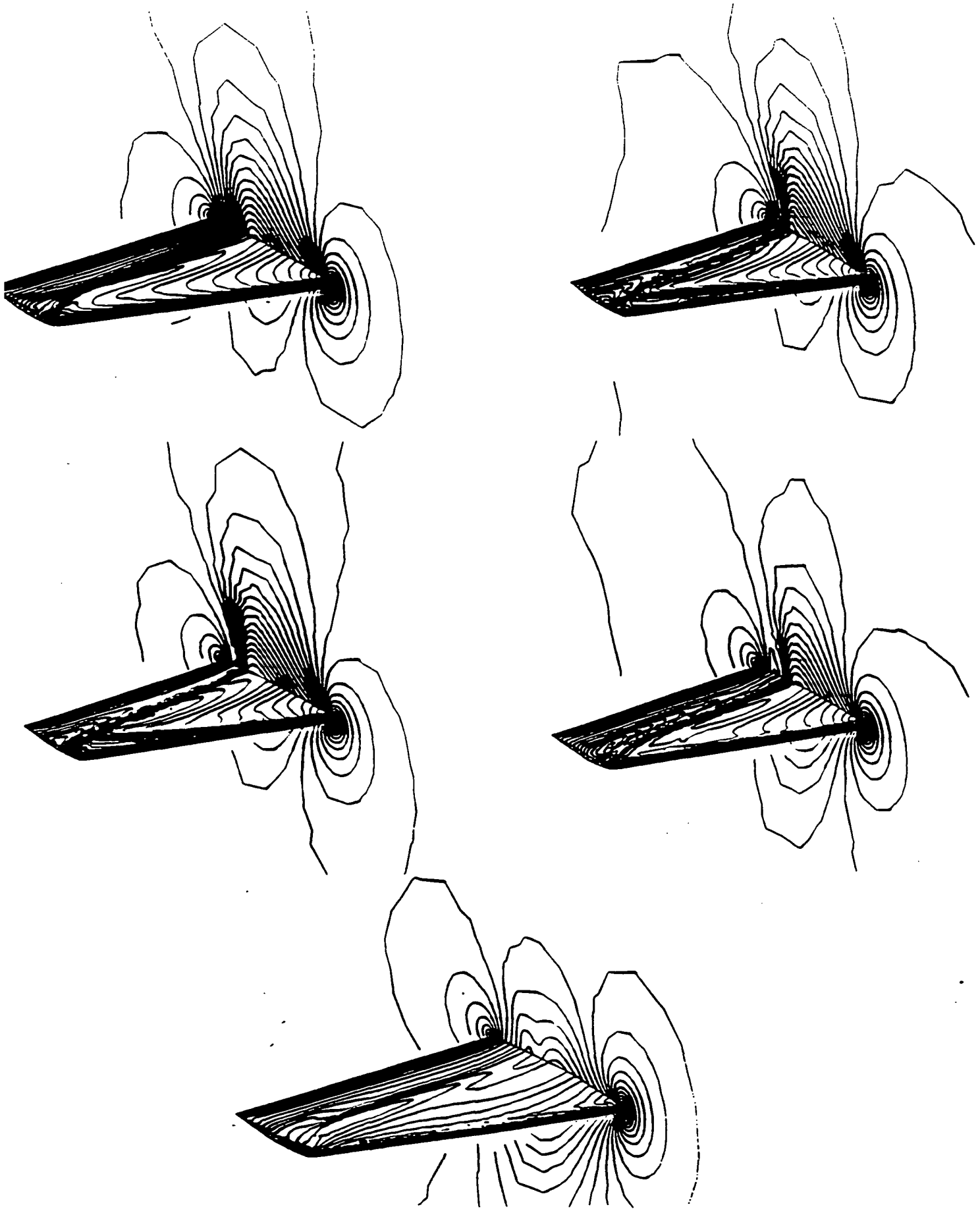

Figure 7

The simulation of inviscid transonic flow over a sinusoidally oscillating ONERA M6 wing. The distribution of the pressure contours on the upper surface of the wing during the initial portion of the cycle.

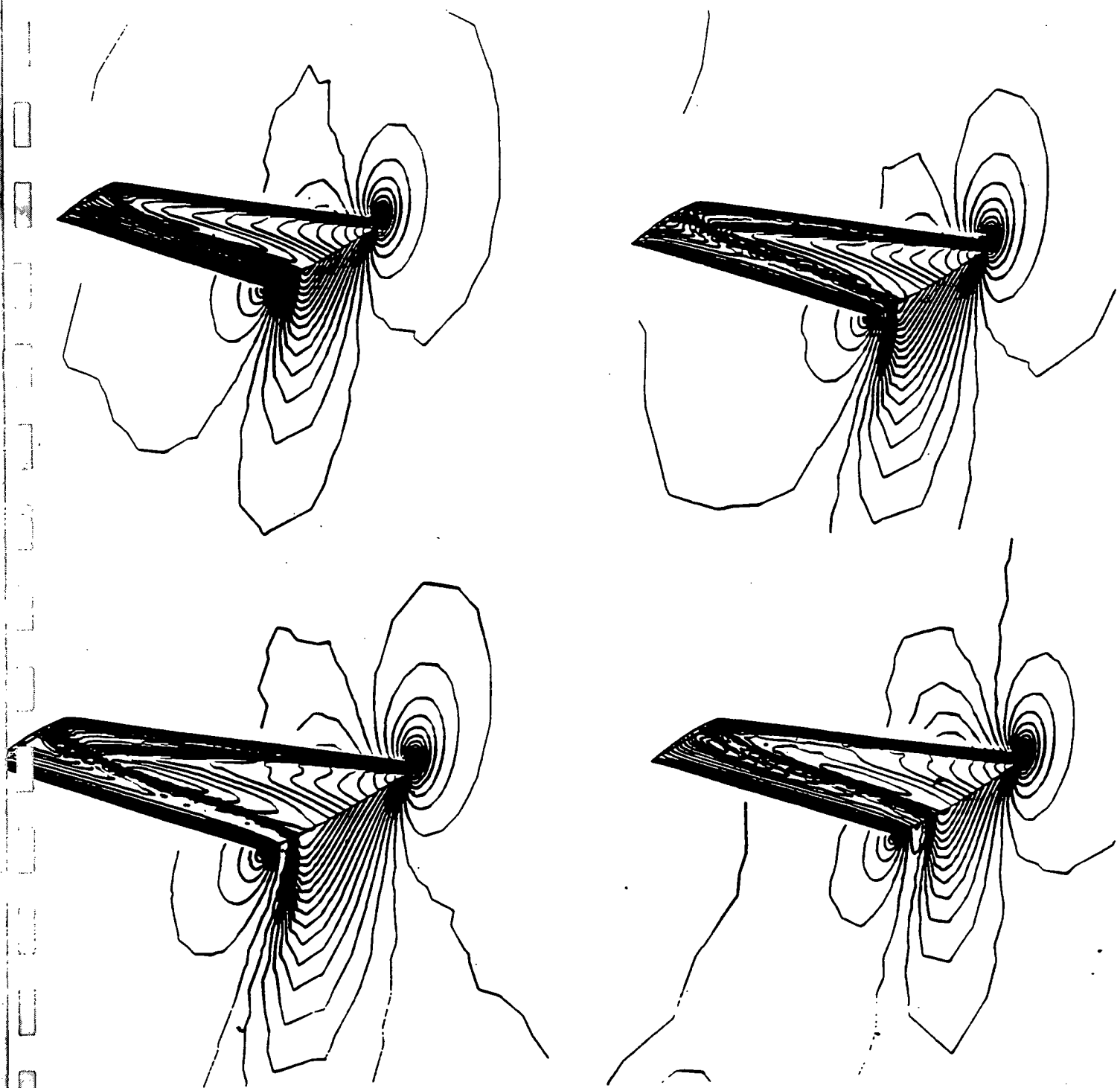

Figure 8

The simulation of inviscid transonic flow over a sinusoidally oscillating ONERA M6 wing. The distribution of the pressure contours on the lower surface of the wing during the latter portion of the cycle.